Contrib Mineral Petrol (2002) 143: 219–235
DOI 10.1007/s00410-001-0336-3

Jörg Hermann

Experimental constraints on phase relations in subducted continental crust

Received: 20 April 2001 / Accepted: 9 November 2001 / Published online: 12 January 2002
© Springer-Verlag 2002

Abstract Synthesis piston cylinder experiments were carried out in the range 2.0–4.5 GPa and 680–1,050 °C to investigate phase relations in subducted continental crust. A model composition (KCMASH) has been used because all major ultrahigh-pressure (UHP) minerals of the whole range of rock types typical for continental crust can be reproduced within this system. The combination of experimental results with phase petrologic constraints permits construction of a UHP petrogenetic grid. The phase relations demonstrate that the most important UHP paragenesis consists of coesite, kyanite, phengite, clinopyroxene, and garnet in subducted continental crust. Below 700 °C talc is stable instead of garnet. As most of these minerals are also stable at much lower pressure and temperature conditions it is thus not easy to recognize UHP metamorphism in subducted crust. A general feature, however, is the absence of feldspars at H_2O-saturated conditions. Plagioclase is never stable at UHP conditions, but K-feldspar can occur in H_2O-undersaturated rocks. Mineral compositions in the experiments are fully buffered by coexisting phases. The Si content of phengite and biotite increase with increasing pressure. At 4.0 GPa, 780 °C, biotite contains 3.28 Si per formula unit, which is most probably caused by solid solution of biotite with talc. Above 800 °C, the $CaAl_2SiO_6$ component in clinopyroxene buffered with kyanite, coesite and a Mg-phase increases with increasing temperature, providing a tool to distinguish between 'cold' and 'hot' eclogites. Up to 10% Ca-eskolaite ($Ca_{0.5}[]_{0.5}AlSi_2O_6$) in clinopyroxene has been found at the highest temperature and pressure investigated (>900 °C, 4.5 GPa). Garnet buffered with coesite, kyanite and clinopyroxene displays an increase of grossular component with increasing pressure for a given temperature. Although the investigated system represents a simplification with respect to natural rocks, it helps to constrain general features of subducted continental crust. The observed phase relations and phase compositions demonstrate that at pressures >3.0 GPa and temperatures >800 °C continental crust can retain significant amounts of H_2O (>1 wt%), whereas K-free mafic or ultramafic rocks are dry at these conditions. UHP parageneses are only preserved if the whole exhumation path is situated within the stability field of phengite, i.e. if there is cooling during exhumation or if the whole exhumation occurred at T <700 °C. In contrast, break down of phengite and concomitant partial melting in terranes that show isothermal decompression may lead to a complete recrystallization of the subducted crust during exhumation. The density of UHP rocks can be estimated on the basis of the established phase relations. Pelitic rocks are likely to have a density close to mantle rocks (3.3 g/cm^3) because of significant amounts of dense garnet and kyanite whereas granitic rocks are less dense (3.0 g/cm^3). Hence, subducted average continental crust is most probably buoyant with respect to mantle rocks and tends to get exhumed as soon as it is detached from the down-going slab. Electronic supplementary material to this paper can be obtained by using the Springer LINK server located at http://dx.doi.org/10.1007/s00410-001-0336-3.

J. Hermann
Research School of Earth Sciences,
Australian National University, 0200 ACT, Australia
E-mail: joerg.hermann@anu.edu.au
Tel.: +61-2-61258842
Fax: +61-2-61255989

Editorial responsibility: J. Hoefs

Introduction

Exhumed high-pressure metamorphosed rocks permit insights in the dynamics of subduction zones and are crucial for the understanding of convergent plate boundaries. It has been long known that mafic rocks can

be metamorphosed into high-pressure eclogites (Eskola 1920). The transition from garnet–plagioclase granulites to eclogites in mafic compositions has been experimentally studied in detail already more than 30 years ago by Green and Ringwood (1967), who recognized that eclogite facies metamorphism occurs during subduction. Experimental studies followed to investigate the phase relations in subducted oceanic lithosphere, i.e. mafic rocks (Poli and Schmidt 1995; Schmidt and Poli 1998) ultramafic rocks (Yamamoto and Akimoto 1977; Ulmer and Trommsdorff 1999) and, to a lesser extent, in pelites (Nichols et al. 1994; Domanik and Holloway 1996; Ono 1998) and granites (Green and Lambert 1965; Huang and Wyllie 1973).

In contrast, ultrahigh-pressure (UHP) coesite facies metamorphism of continental crust was discovered less than 20 years ago when coesite was found in the Dora Maira Massif, Alps (Chopin 1984). This provides evidence that continental crust was subducted to 100 km depth and was later exhumed. Sobolev and Shatsky (1990) reported diamonds from metamorphic gneisses. This implies that the continental crust reached a depth of at least 150 km. These findings drastically changed the ideas of geologists concerning the limits of crustal metamorphism. Besides the critical minerals, such as diamond and coesite to prove UHP metamorphism, very little is known about the phase relations that occur in subducted continental crust in UHP conditions. There exist experiments on the stability of mineral assemblages, mainly in the synthetic $MgO–Al_2O_3–SiO_2–H_2O$ (Schreyer 1988) and $K_2O–MgO–Al_2O_3–SiO_2–H_2O$ (Massone and Schreyer 1987, 1989; Massone and Szpurzka 1997) systems as well as some information of natural crustal rocks at UHP conditions (Huang and Wyllie 1973; Stern and Wyllie 1973; Ono 1998; Patiño Douce and McCarthy 1998; Domanik and Holloway 2000), but there is still a great necessity to enlarge the existing data set in order to recognize and quantify eclogite facies metamorphism in continental crust (Harley and Carswell 1995).

In this paper, the model system $K_2O–CaO–MgO–Al_2O_3–SiO_2–H_2O$ (KCMASH) has been chosen to study the behaviour of subducted continental crust and oceanic sediments because it represents the simplest possible system to produce the main mineral assemblages in UHP mafic, pelitic and granitic rocks. With respect to natural systems, the major difference is the absence of Na and Fe. However, at UHP conditions Na is incorporated in clinopyroxene and Fe is distributed among the Mg phases and, hence, these elements do not produce additional phases. It is the purpose of this paper to provide basic phase relations of subducted continental crust based on experiments and phase petrology. The established stability fields of UHP parageneses in the investigated system permit recognition of subducted continental crust. Special emphasis is placed on the stability of hydrous phases, which are able to transport H_2O to mantle depth. The changes in composition of fully buffered UHP minerals with pressure (P) and temperature (T) are reported. These compositional changes help to estimate metamorphic conditions in subducted crust. The experimental phase relations are applied to analyses of hydration and dehydration reactions and to questions of preservation of high-pressure mineral assemblages during exhumation of subducted continental crust.

Experimental and analytical techniques

Existing experiments between 3–6 GPa, 700–1,000 °C in natural systems (Huang and Wyllie 1973; Nichols et al. 1994; Poli and Schmidt 1995; Ono 1998; Patiño Douce and McCarthy 1998; Domanik and Holloway 2000), as well as UHP parageneses in mafic, pelitic and granitic rocks of the Dora Maira Massif (Compagnoni et al. 1995), display a very limited range of major minerals consisting of lawsonite, zoisite, coesite, phengite, biotite, K-feldspar, clinopyroxene, kyanite and garnet. The chosen bulk system $K_2O–CaO–MgO–Al_2O_3–SiO_2–H_2O$ (KCMASH) for the experiments represents the simplest chemical system to produce all these minerals. The oxide proportions were selected in order to obtain saturation of kyanite and quartz/coesite in all experiments, and similar amounts of the high-pressure phases garnet, clinopyroxene and phengite (Fig. 1a). Additionally the proportions ensure that phengite composition is not limited by the chosen bulk composition. Consequently, the resulting bulk rock composition represents a mixture between a mafic end member (in order to produce garnet and clinopyroxene) and a pelitic end member (to produce kyanite, coesite and a K-phase) and does not represent a natural composition.

The starting material, P1 (Table 1), was prepared as a gel, which was fused to a glass at 1,400 °C. A combination of key trace elements was added at a 100–350 ppm level (Hermann and Green 2001), which resulted in the presence of accessory allanite in most of the experiments. These trace elements were used to study residue-partial melt partitioning in the higher temperature range of the investigated system (Hermann and Green 2001). P1b consists of a sintered oxide mix with addition of natural Mg-phengite and Mg-talc and has the same major element composition as P1. In this set of experiments, the ~10-μm phengite only partially reacted in the 200-h run and never changed its composition completely , indicating that for the investigated P–T range and experimental time the diffusion is too slow to change the already existing phase compositions. Therefore, the best way of investigating the phase relations at such low temperatures is by synthesis experiments. The experiments were always saturated in H_2O to enhance reaction rates at the low experimental temperatures, but not so H_2O-rich as to risk losing the solid K-phases by solubility of components in the liquid at significantly lower temperatures than their breakdown reaction.

Internal consistency and attainment of equilibrium was tested in several ways. (1) All experiments satisfy the phase rule indicating that there are no metastable phases present (see below). (2) Schreinemaker's rule combined with the chemography provides constraints on the possible distribution of phases. (3) Phase compositions are fully buffered in most experimental parageneses and must change systematically with pressure and temperature. Additionally, some of the experiments were repeated at the same conditions to check reproducibility. Apart from clinopyroxene, which displays commonly significant zoning in Al contents, the synthesized phases were of homogenous composition. All these observations indicate that the experiments most probably reached equilibrium.

Synthesis experiments were run in end-loaded 1.27-cm piston-cylinder apparatuses. Pressure was calculated from direct conversion of load to pressure in the low friction experiments using salt sleeves and Teflon foil and is accurate to ± 0.1 GPa. Temperature was controlled using type B thermocouples ($Pt_{94}Rh_6/Pt_{70}Rh_{30}$) and is accurate to ± 10 °C. Details about the experimental procedure are given in Hermann and Green (2001).

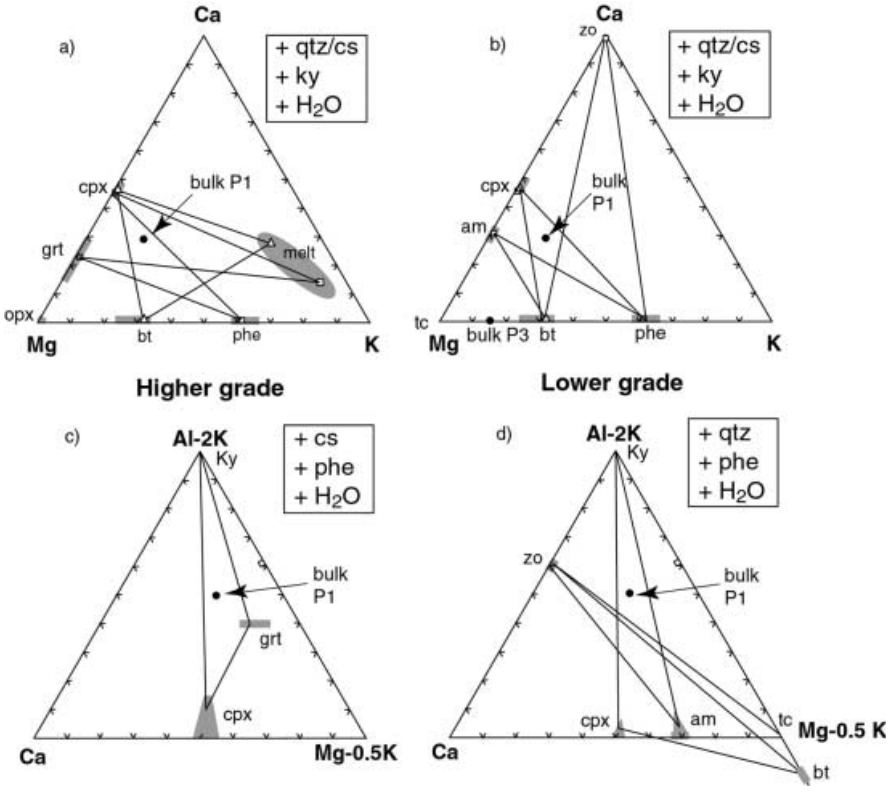

Fig. 1a–d. Chemography at higher grade (**a**, **c**) and lower grade (**b**, **d**) conditions for the investigated system. The range of phase compositions is indicated by *grey bars*, individual phase composition of single analyses is given in *symbols*. The position of the bulk with respect to the phases determines which phases are completely consumed during the univariant reactions (Fig. 9). An ideal phengite composition with Si = 3.5 was used for projections in **c** and **d**. For abbreviations see Table 2

Phase relations were analyzed in polished mounts by back-scattered electron images on a JEOL 6400 SEM (Electron Microscopy Unit, ANU). The phase compositions were determined using an energy dispersive detector, and acceleration voltage of 15 kV and a beam current of 1 nA. The K_2O content of micas did not differ significantly by using area scans or spot analyses indicating that the micas were stable under the low beam current and that there was no significant K_2O loss during analyses.

Experimental results

The synthesized phase assemblages and the experimental conditions are presented in Table 2 and the results are plotted in Fig. 2. Most of the experiments produced 5–20-μm-sized minerals with nice crystal shapes (Fig. 3). Grain boundaries between minerals are generally straight and indicate that the minerals attained textural equilibrium. Eleven solid major phases were found over the whole investigated P–T range (Table 2, Fig. 2). A SiO_2 phase, coesite or quartz, and kyanite were produced in all experiments. Several hydrous phases are stable in the investigated grid. Zoisite and amphibole (Fig. 3a) have very similar, restricted stability fields at a maximum of ~800 °C and ~3 GPa. Biotite (Fig. 3b) has the highest thermal stability at pressures lower than 3.0 GPa and was found at up to 780 °C, 3.9 GPa. Talc (Fig. 3c) is stable at temperatures below ~730 °C and the upper stability in pressure was not reached at 4.45 GPa. Phengite (Fig. 3d, e) has the largest stability field at high pressure and temperature. The transition from orthopyroxene- to garnet-bearing parageneses is the least precise in the whole grid as both phases occur together in a transition interval of about 50 °C (Fig. 2). Experiments at 3.5 GPa, 850 °C, 4.0 GPa, 750 °C and 4.2 GPa contain orthopyroxene coexistent with kyanite (Fig. 3f), but without garnet. The quite wide transition of orthopyroxene to garnet could result from problems in nucleation of garnet. To test this hypothesis, a mix of talc, kyanite and phengite was blended with seeds of 98% pure pyrope and run at 4.0 GPa, 780 °C. There was no garnet growth observable, but high amounts of orthopyroxene (~25%) coexisting with kyanite. The seeds were mainly dissolved and the few grains still present preserved 5% almandine and 5% grossular component, which represent impurities of the starting garnet. These

Table 1. Oxide proportions of the starting materials. In P1, different amounts of H_2O (Table 2) were added using a microlitre syringe. Natural Mg-phengite and talc are blended with a sintered CAS-oxide mix in P1b. $Al(OH)_3$ is the H_2O source in the oxide mix P1c. The desired amount of H_2O in various experiments labeled with P1c′ (Table 2) was obtained by blending P1c and P1 mixes in different proportions. P3 consist of a mix of natural minerals with 50 wt% talc, 20% phengite, 25% kyanite and 5% pyrope. P1 has traces of Na_2O (~0.2 wt%), P1b and P3 contain traces of FeO and TiO_2 derived from the natural minerals

	P1	P1b	P1c	P3
SiO_2	61.5	60.5	55.8	53.9
Al_2O_3	21.0	20.5	18.9	21.6
MgO	8.0	7.8	7.2	18.3
CaO	6.0	5.9	5.4	0.1
K_2O	3.0	2.9	2.7	2.3
H_2O	–	2.2	10	3.3

Table 2. Experimental run conditions and products. Phases in *bold* occur at 10–50%, others at 1–10%. *Italics* refer to accessory minerals (< 1%). Phases in *parenthesis* are stabilized by traces of Ti and Fe, which occur in the natural phengite and talc used in the P1b starting material and are not considered as stable phases in the KCMASH system. *P* Pressure; *T* temperature; *h* time in h; *Cs* coesite; *Qtz* quartz; *Phe* phengite; *Cpx* clinopyroxene; *Opx* orthopyroxene; *Grt* garnet; *Ky* kyanite; *Bt* biotite; *Tc* talc; *Zo* zoisite; *Am* amphibole; *All* allanite; *M* melt; *F* fluid; *L* liquid

Run no.	Mix	P (GPa)	T (°C)	Time (h)	H_2O (wt%)	Phases
C-797	P1	3.5	720	640	10.3	**Cpx**, **Cs**, **Phe**, **Tc**, **Ky**, F, *All*
C-810[a]	P1	3.5	900	187	2.6	**Cpx**, **Cs**, **Phe**, **Grt**, **Ky**, **Melt**, Opx, *All*
C-825[a]	P1	3.5	950	304	2.5	**Cpx**, **Cs**, **Phe**, **Grt**, **Ky**, **Melt**, *All*
C-879[a]	P1	3.5	850	155	5.3	**Cpx**, **Cs**, **Phe**, **Opx**, **Ky**, **Melt**, *All*
C-896[a]	P1	3.5	1,000	99	2.9	**Cpx**, **Cs**, **Grt**, **Ky**, **Melt**, *All*
C-905	P1	3.0	1,000	95	2.7	**Cpx**, **Cs**, **Grt**, **Ky**, **Melt**, Opx
C-914	P1	3.0	730	502	8.9	**Cs**, **Phe**, **Ky**, **Zo**, **Am**, F
C-929[a]	P1b	2.0	900	140	2.2	**Cpx**, **Qtz**, **Bt**, **Melt**, Opx, Ky, (Grt)
C-930	P1b	3.0	800	192	2.2	**Cpx**, **Cs**, **Phe**, **Bt**, **Ky**, Zo-All, Melt
C-933	P1b	3.5	800	190	2.2	**Cpx**, **Cs**, **Phe**, **Bt**, **Ky**, F
C-934[a]	P1b	2.5	1,000	189	2.2	**Cpx**, **Qtz**, **Grt**, **Melt**, (Bt)
C-936[a]	P1	3.0	900	240	3.5	**Cpx**, **Cs**, **Grt**, **Ky**, **Melt**, **Opx**, Phe, Bt, *All*
C-940[a]	P1b	2.0	1,000	163	2.2	**Cpx**, **Qtz**, **Grt**, **Melt**, Opx
C-941	P1c'	3.2	760	192	4.5	**Cpx**, **Cs**, **Phe**, **Bt**, **Ky**, F, *All*
C-942[a]	P1c'	2.5	840	80	4.5	**Cpx**, **Qtz**, **Ky**, **Bt**, **Melt**, All
C-950	P1c'	2.0	730	240	5.5	**Qtz**, **Ky**, **Bt**, **Am**, **Zo**, Melt
UHP 50[a]	P1c'	4.52	1,000	72	2.5	**Cpx**, **Cs**, **Phe**, **Grt**, **Ky**, **Melt**, *All*
C-954	P1c'	2.5	730	233	5.5	**Qtz**, **Ky**, **Phe**, **Bt**, **Zo**, **Tc**, Am, F
C-976	P1c'	2.5	800	198	4.5	**Cpx**, **Qtz**, **Ky**, **Phe**, **Bt**, **Zo**, F
C-982[a]	P1c'	2.5	950	165	2.5	**Cpx**, **Qtz**, **Ky**, **Opx**, **Grt**, **Melt**, *All*
C-983[a]	P1c'	3.0	950	168	2.5	**Cpx**, **Cs**, **Ky**, **Grt**, **Melt**, Opx, *All*
UHP 56[a]	P1c'	4.05	1,000	72	2.5	**Cpx**, **Cs**, **Phe**, **Grt**, **Ky**, Melt, *All*
C-988[a]	P1c'	2.0	850	266	2.5	**Cpx**, **Qtz**, **Bt**, **Ky**, Czo/All, Melt
C-989[a]	P1c'	3.0	850	264	2.5	**Cpx**, **Cs**, **Phe**, **Bt**, **Ky**, Melt?, *All*
C-995	P1c'	2.25	760	239	4.0	**Qtz**, **Ky**, **Bt**, **Zo**, **Am**, Melt
C-996	P1c'	2.0	800	239	4.0	**Qtz**, **Ky**, **Bt**, **Zo**, **Am,** Melt
C-1080[a]	P1c'	2.5	900	187	2.5	**Cpx**, **Qtz**, **Bt**, **Ky**, Melt?, *All*
C-1093	P1c'	4.2	780	169	2.5	**Cpx**, **Cs**, **Phe**, **Opx**, **Ky**, F, *All*
C-1109	P1c'	4.5	800	123	4.0	**Cpx**, **Cs**, **Phe**, **Opx**, **Grt**, **Ky**, F, *All*
C-1115[a]	P1c'	4.5	1,050	73	2.7	**Cs**, **Grt**, **Ky**, **Melt**, Cpx, *All*
C-1119	P1	2.5	680	230	3.8	**Qtz**, **Ky**, **Phe**, **Zo**, **Tc**, F
C-1121	P1c'	4.5	900	123	2.5	**Cpx**, **Cs**, **Phe**, **Grt**, **Ky**, F, *All*
C-1125	P1c'	4.0	900	190	2.5	**Cpx**, **Cs**, **Phe**, **Grt**, **Ky**, Melt, *All*
C-1202	P1c'	4.0	750	170	6.0	**Cpx**, **Cs**, **Phe**, **Opx**, **Ky**, F, *All*
C-1203	P3	4.0	780	200	3.3	**Cs**, **Bt**, **Opx**, **Ky**, F
C-1220	P1c'	4.45	850	162	5.0	**Cpx,** **Cs**, **Phe**, **Grt**, **Ky**, F, *All*
C-1223	P1c'	4.45	700	100	6.0	**Cpx**, **Cs**, **Phe**, **Ky**, **Tc**, F

[a]Melt compositions of experiments are reported in Hermann and Green (2001)

observations indicate that the high-pressure orthopyroxene field cannot be explained by inhibition of garnet nucleation. Moreover, this experiment strongly suggests that at 4.0 GPa the reaction talc → orthopyroxene + coesite + liquid occurs.

All experiments were performed with a small amount of excess H_2O not bound in the hydrous phases. The additional H_2O produced a hydrous granitic melt, coexisting with hydrous phases at relatively higher temperature (Fig. 2). The H_2O content of hydrous granitic melts (for determination see Hermann and Green 2001) gradually increases with decreasing temperature. The highest estimated H_2O content of ~25% in a quenchable melt was found at 730 °C, 2 GPa. At 3.5 GPa, quenchable melt was found down to 850 °C with a H_2O content of ~15%. At relatively lower temperature, cavities were observed between phases (Fig. 3c), which contained a Si and Al rich precipitate with minor K. This indicates that an aqueous solute-rich fluid was present in these experiments, which separated into small precipitates (Fig. 3d) and water during quenching. The analyses of experimental results indicate that the transition from melt to non-quenchable liquid (Fig. 2) appears at an estimated H_2O content of about 20–30%. It is important to note that this transition does not correspond to the solidus in the investigated system; rather, it reflects the quench behaviour of liquids at high pressure as a function of the amounts of dissolved H_2O.

Phase composition

The phase compositions obtained in the experiments are available as electronic tables (see Tables 1–5 in electronic supplementary material). The compositions of all components in the phases are buffered and, consequently,

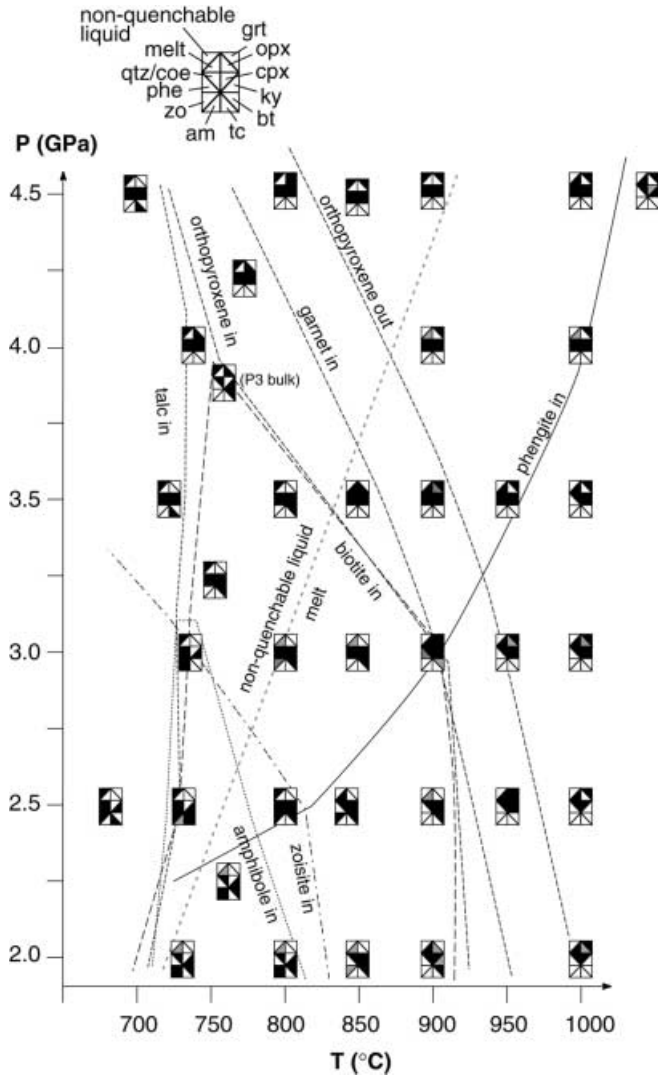

Fig. 2. Experimental results in the P–T space and the stability fields of hydrous phases. Major phases are shown in *black* and minor phases are given in *grey* as defined in Table 2. The transition of non-quenchable liquid to melt occurs at an estimated H_2O content of about 25–30% in the liquid phase and does not represent the solidus of the investigated system

phases with solid solutions should change their composition as a function of temperature and pressure. It is important to note that all observed trends are obtained for samples buffered with kyanite and coesite/quartz. The potential of phases to record UHP metamorphic conditions is examined and the experimentally obtained compositions are compared with other experimental studies and minerals from high-pressure metamorphic rocks.

Phengite

Phengite results from solid solution between muscovite [K[]$Al_3Si_3O_{10}(OH_2)$] and celadonite [K[]$MgAlSi_4O_{10}(OH_2)$] and can be characterized by an inverse tschermak exchange $MgSiAl_{-2}$ starting from muscovite. The amount of celadonite is thus easily visible in the Si content of phengite, which strongly increases with increasing pressure (Fig. 4a). The highest Si content of 3.63 was found at the low T, high P end of the investigated grid. Si isopleths of phengite coexisting with garnet have a positive slope in the P–T space. The Si isopleths are nearly horizontal when phengite coexists with biotite, orthopyroxene or talc (Fig. 4b). The Mg content of phengite is always higher than required by the pure celadonite substitution indicating a higher octahedral occupancy than normal white mica. This feature can be interpreted as a biotite solid solution in phengite (Fig. 4c). In phengite coexisting with biotite, the octahedral occupancy in phengite increases with increasing temperature and reaches nearly 20% biotite component at 900 °C and 3.0 GPa. At higher pressure, where biotite is not stable, the octahedral occupancy decreases and the biotite component in phengite is less than 5% above 4.0 GPa.

The strong variation of phengite compositions as a function of pressure confirms the importance of this mineral for determination of UHP metamorphism (Massone and Schreyer 1987, 1989; Massone and Szpurzka 1997). The different slopes of Si isopleths in different parageneses is in agreement with previous experiments, which show that Si isopleths of phengite coexisting with talc are temperature independent (Massone and Schreyer 1989), but are sensitive to temperature when phengite is in paragenesis with garnet (Green and Hellman 1982; Massone and Szpurzka 1997). Thus, it is crucial to establish the correct paragenesis for application of any Si-isopleth barometry. A detailed application of phengite barometry on white schists will be presented elsewhere.

Biotite

Similarly to phengite, biotite displays a strong variation in Si content with pressure (Fig. 5a). With increasing temperature, the Si content decreases only slightly, indicating a gentle positive slope of Si isopleths in P–T space (Fig. 5b). Above 2.5 GPa, Si contents exceeds 3.0, which is the upper limit of pure phlogopite, and reaches a maximum of 3.28 at the upper pressure limit of the biotite stability field at 4.0 GPa (Fig. 5b). The increase in Si content is coupled with a systematic decrease in K content indicating a $[]SiK_{-1}Al_{-1}$ exchange. This suggests that the observed Si increase in UHP biotite is caused by solid solution with talc rather than with phengite (Fig. 5c). This is supported by the Si–Al variation diagram (Fig. 5d) showing that the whole range of measured biotites can be explained by the end members eastonite, talc and minor muscovite.

Biotite is so far unknown as indicator of UHP metamorphism in SiO_2-saturated rocks. This study demonstrates that, at least in Fe-free compositions, the Si content of biotite can be used to estimate metamor-

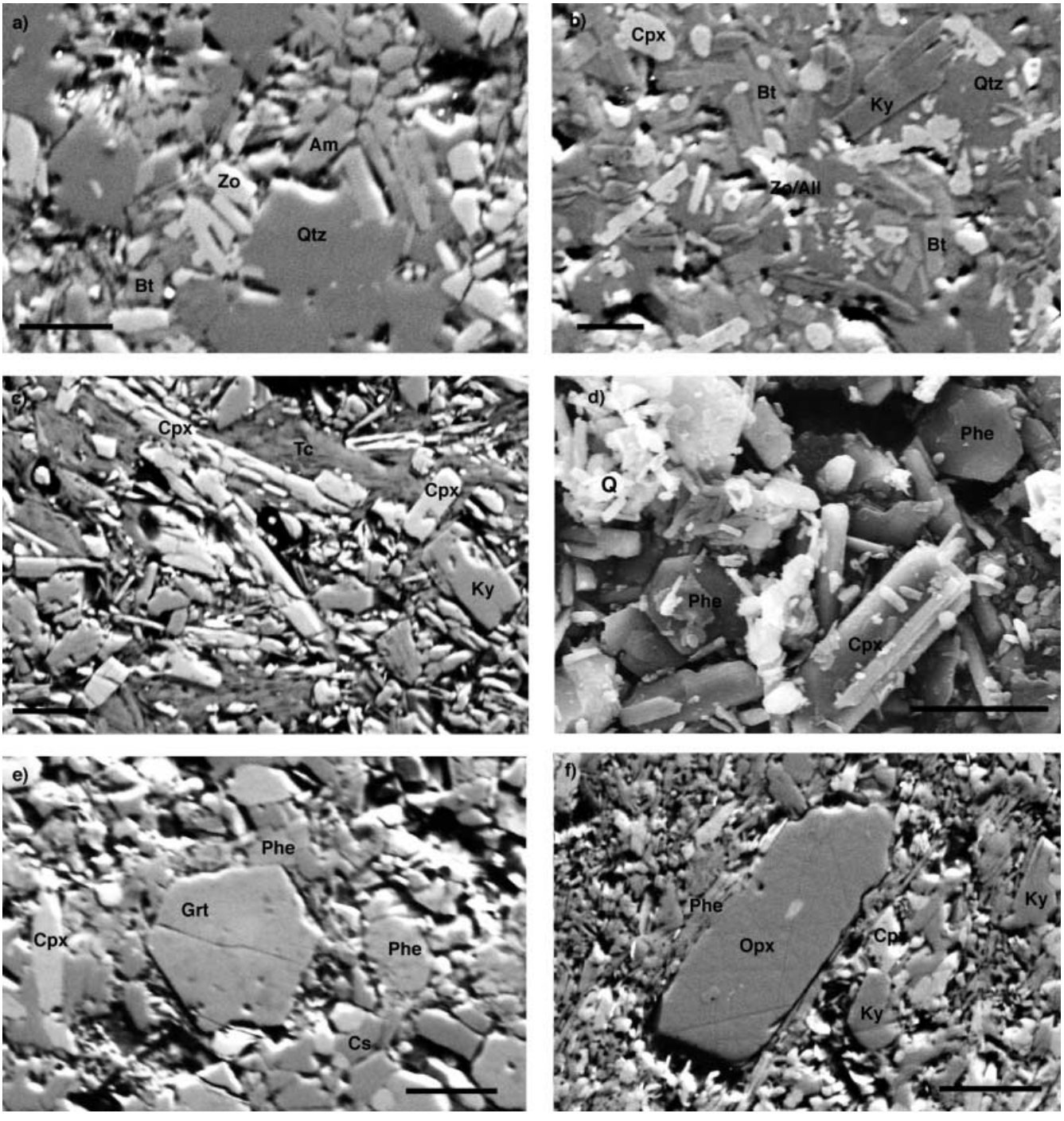

Fig. 3. Back-scatter electron and secondary electron (**d)** images of run products. *Scale bars* represent 10 μm. **a** Three hydrous phases, amphibole, zoisite and biotite, coexist at 760 °C and 2.25 GPa (C-995). **b** Biotite is stable to higher temperatures than phengite (850 °C, 2.0 GPa). At the reaction of zoisite to clinopyroxene, zoisite incorporates trace elements to form allanite (C-988). **c** Talc coexists with kyanite and phengite (not visible) at 700 °C, 4.45 GPa (C-1223). **d** SEM image of run C-797 (720 °C, 3.5 GPa) displays idiomorphic flakes of phengite and well-crystallized clinopyroxene. The coexisting liquids separates into water and quench products (*Q*) during quenching of the run. **e** The typical UHP paragenesis in crustal rocks consist of garnet, phengite, coesite, clinopyroxene and kyanite (not visible; C-1121, 900 °C, 4.5 GPa). **f** In the Fe-free system, orthopyroxene is a high-pressure phase and coexists with kyanite (C-1093, 780 °C, 4.2 GPa)

phic pressure. Biotite in ultramafic compositions (Konzett and Ulmer 1999) and coexisting with orthopyroxene (Sato et al. 1997) display a Si content >3.0 above 6.0 GPa at 1,100 and 1,300 °C, respectively. However, biotite in these experiments is not buffered with coesite and, hence, the responsible substitution is likely to be different. Based on X-ray diffraction data from experiments, Massone and Schreyer (1987) proposed that biotite coexisting with K-feldspar, phengite and quartz is eastonite at low pressures (0.5 GPa) and displays an increase in Si content with increasing pressure, in

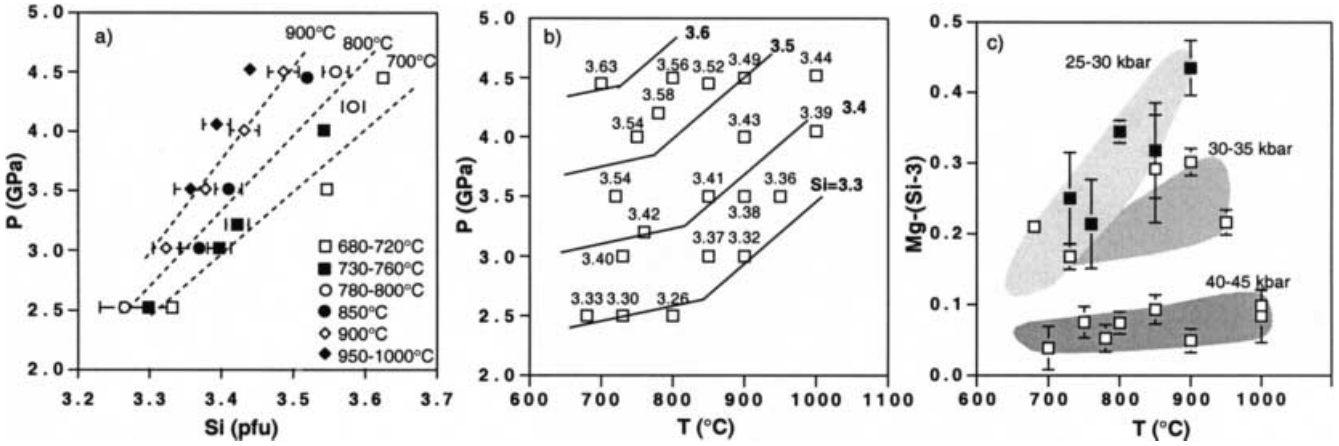

Fig. 4a–c. Composition of experimentally determined phengite. Error bars refer to 1σ errors of several analyses in the same experiment. **a** Increase in Si per formula unit (normalized on 22 charges) content in phengite with increasing pressure at different temperatures. The error on Si contents in phengite derived from normalization because of possibly low K-contents is smaller than the indicated *error bar*. **b** Si contents of phengite in single experiments and Si contours in P–T space. The isotherms **a** and isopleths **b** are eyeball fits to the experimental data. **c** The amount of Mg in phengite exceeding the required amount by the celadonite content (Si-3) increases with temperature in phengite coexisting with biotite (*filled squares*)

agreement with the results reported here. Experiments in a metagreywacke produced biotite with Si = 3.04 buffered with quartz, but without kyanite at 3.0 GPa, 1,000 °C (Patiño Douce and McCarthy 1998). Schertl et al. (1991) reported low K phlogopites with Si > 3 coexisting with kyanite from white schists of the Dora Maira Massif as prograde inclusion in garnet. The experiments suggest that this phlogopite formed at pressure of about 3.0 GPa, which is in agreement with the observation that the white schists were in the coesite

Fig. 5a–d. Composition of experimentally determined biotite. *Error bars* refer to 1σ errors of several analyses in the same experiment. **a** Increase in Si content per formula unit (normalized on 22 charges) in biotite with increasing pressure at different temperatures. Note that most of the biotites contain more than 3 Si (pfu). **b** Si contents of phengite in single experiments and Si contours in P–T space. The isotherms **a** and isopleths **b** are eyeball fits to the experimental data. **c** The decreasing K content with increasing Si content in biotite indicates that solid solution of talc with biotite is most likely responsible for the high Si content in biotite. **d** Variation in Si and Al of biotite can be explained by solid solution of end members eastonite, talc and muscovite

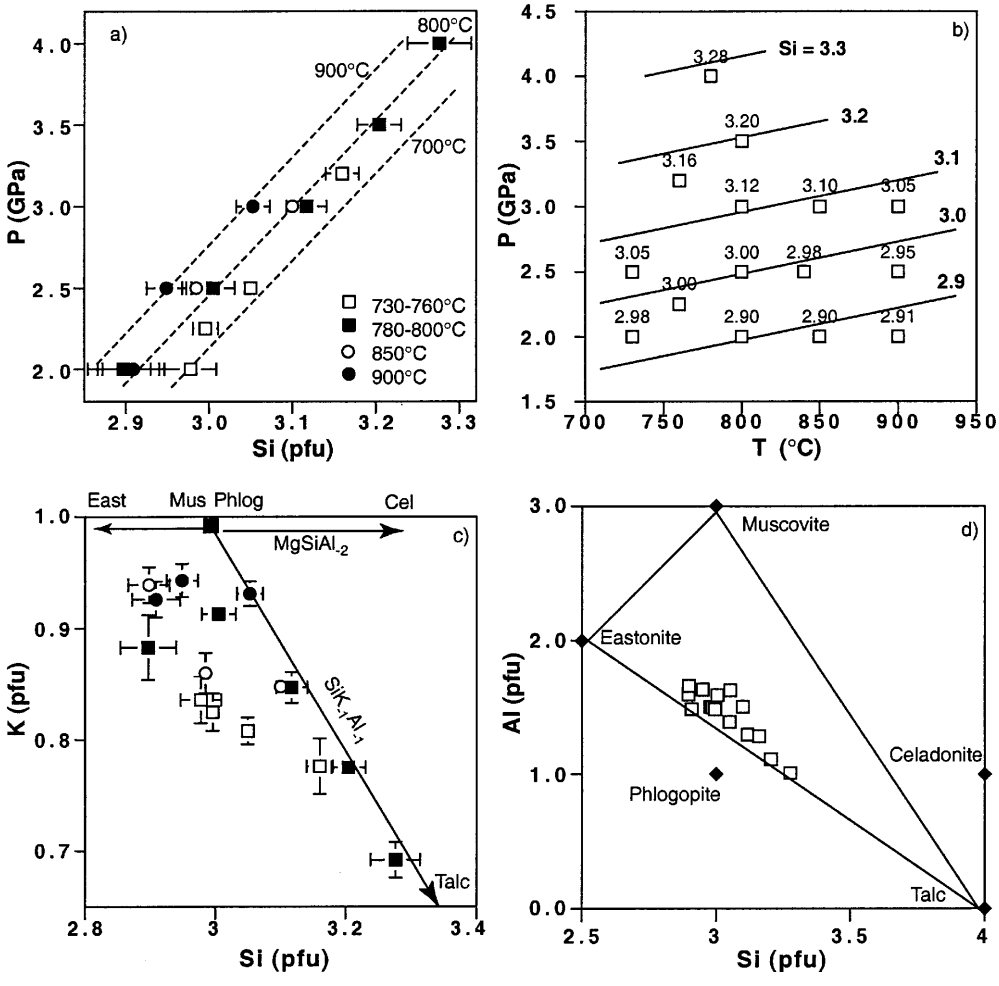

stability field. Biotite inclusions in garnet-hosting metamorphic micro diamonds from gneisses of the Kokchetav Massif, Kazakhstan, have been regarded to form at UHP conditions (Shatsky et al. 1995; Zhang et al. 1997). Such biotite has a Si content of 2.8–2.9, which is very similar to biotite formed in the granulite facies overprint. It is suggested that biotite with a Si content of < 3 is unlikely to be a UHP-phase in normal pelitic compositions.

Clinopyroxene

The Si content of clinopyroxene decreases whereas the Al content increases suggesting an increasing tschermak exchange $Al_2Mg_{-1}Si_{-1}$ with increasing temperature (Fig. 6a). The Ca content decreases with increasing temperature mainly because of solid solution with orthopyroxene (up to 10% at 1,000 °C). The pressure effect on clinopyroxene composition is much smaller. The Si content increases and the Al content decreases slightly at a fixed temperature with increasing pressure. Most of the clinopyroxenes display cation deficiency. The total cations decrease systematically with excess Al on the octahedral site, which is defined by Al neither bound in a Ca-tschermak ($CaAlAlSiO_6$) nor in jadeite ($NaAlSi_2O_6$) component. The good correlation of excess Al to cation deficiency in the ratio 2:1 suggests the presence of up to 10% Ca-eskolaite ($Ca_{0.5}[]_{0.5}AlSi_2O_6$) in clinopyroxene (Fig. 6b). Because of the large error in determination of excess Al, it is difficult to establish a clear trend. However, it seems that the highest Ca-eskolaite contents occur in samples at high temperature and high pressure (Fig. 6c). A $>10\%$ Ca-eskolaite component results in a decrease of 0.05 Ca (pfu) in the clinopyroxene formula. The measured Ca values at 1,000 °C display a cluster at 2.0–3.0 GPa with 10% orthopyroxene component and no Ca-eskolaite contents, and a cluster with 0.05 Ca (pfu) lower values for the higher pressure range 3.5–4.5 GPa because of additional Ca-

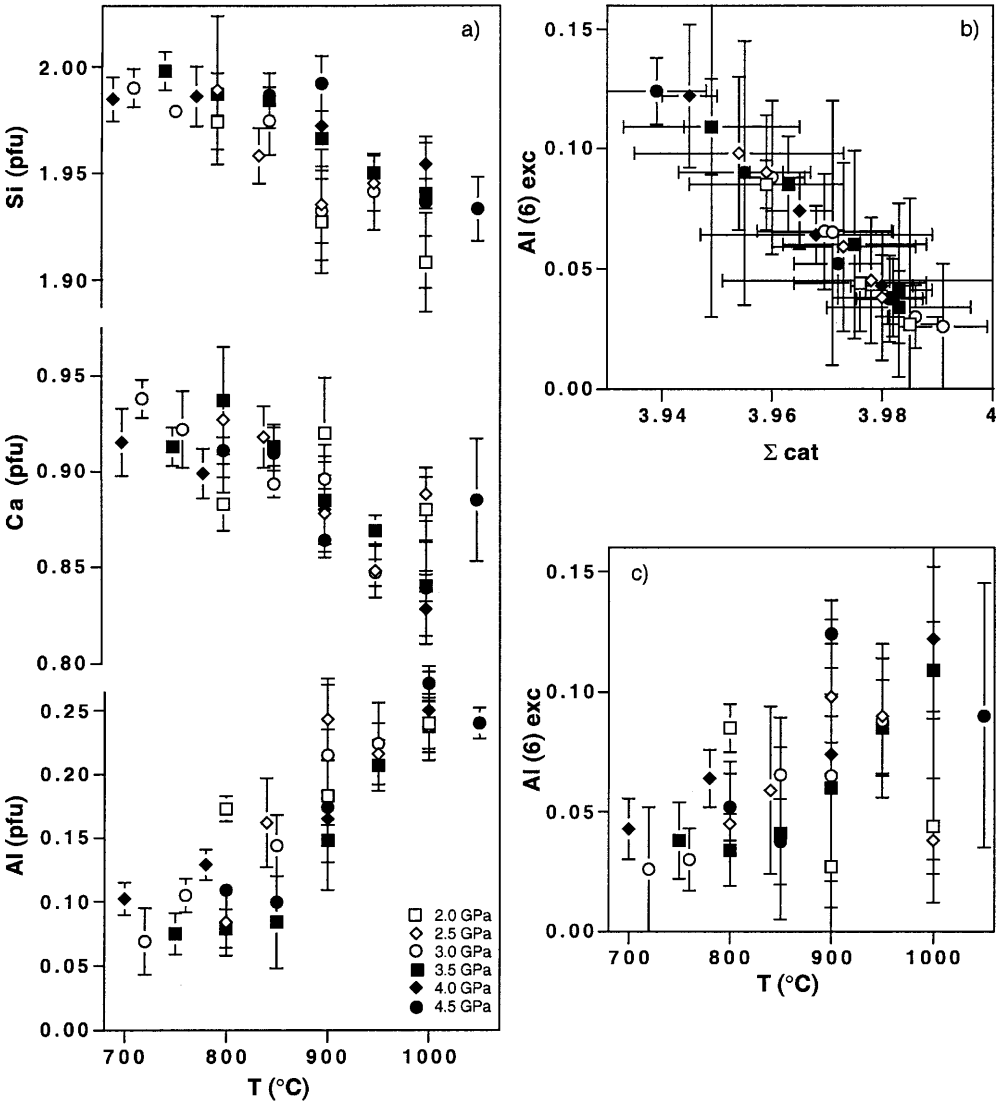

Fig. 6a–c. Composition of experimentally determined clinopyroxene in equilibrium with kyanite and coesite/quartz. *Error bars* refer to 1σ errors of several analyses in the same experiment. **a** Variation of cations (normalized on 12 charges) with temperature. **b** With decreasing total cations, the amount of excess Al on the octahedral site [Al 6 exc = Al(tot)–Na–2×(2-Si)] increases indicating the possible presence of Ca-eskolaite ($Ca_{0.5-0.5}AlSi_2O_6$) in clinopyroxene. **c** Ca-eskolaite component can only be postulated in high temperature, high-pressure experiments. Errors in **b** and **c** refer to 1σ errors on Al content

eskolaite contents. In the whole investigated P–T space there is no significant incorporation of K in clinopyroxene (< 0.2 wt%). There is no systematic change of K with pressure and temperature, indicating that, at least in some samples, detected K is probably a result of small amounts of mica or melt inclusions in clinopyroxene.

The increasing amount of Ca-tschermak component in clinopyroxene buffered with kyanite and coesite with increasing temperature is a useful tool to distinguish between high temperature and intermediate to low temperature eclogites. Omphacite from the Dabie Mountains formed at 600–800 °C, and does not display any Ca-tschermak component (Carswell et al. 1997). This is in agreement with absence of Ca-tschermak component in omphacites from the UHP unit of the Dora Maira Massif (Kienast et al. 1991), where peak metamorphism reached temperatures around 750 °C. On the other hand, UHP omphacite inclusions in zircon from the Kokchetav Massif formed at temperatures ~950 °C and contain ~5–10% of Ca-tschermak component (Shatsky et al. 1995; Hermann et al. 2001), which is in agreement with the experimentally determined amount in the Na-free system.

Clinopyroxene from coesite–kyanite eclogites from the Roberts Victor kimberlite display about 0.25–0.30 more Al (pfu) than needed for the jadeite component (Schulze et al. 2000). Normalization of the reported analyses reveals that these pyroxenes contain about 15–20% Ca-eskolaite and about 5% Ca-tschermaks components. The conditions of formation of the xenoliths are estimated to be about 1,100 °C and 5.0 GPa (Carswell et al. 1981). These data confirm the trend observed in the experiments that the Ca-eskolaite component is increasingly important at high temperature and pressure. Quartz exsolution lamellae in omphacites from UHP eclogites provide evidence for the Ca-eskolaite component in subducted continental crust. For example, omphacites from the Erzgebirge experienced metamorphic conditions of 850 °C and P > 3.3 GPa, and displays about 8% of the Ca-eskolaite component (Schmädicke and Müller 2000). Even higher amounts of the Ca-eskolaite component (~12%) are reported from omphacite included in zircons from the diamond facies eclogites (P = 4.5 GPa, T ~950 °C) of the Kokchetav Massif in Kazakhsthan (Katayama et al. 2000a). These data agree with the experimental results, suggesting that at 4.5 GPa and 900–1,000 °C there is up to 10% of the Ca-eskolaite component in clinopyroxene coexisting with coesite. There is no Ca-eskolaite component in omphacites from kyanite eclogites (Kienast et al. 1991) from the Dora Maira Massif (P ~4.0 GPa, 750 °C). This is in line with the general trend of the experiments showing that both elevated pressure and temperature are needed to produce the Ca-eskolaite component in clinopyroxene.

The observed trends in Ca-tschermak and Ca-eskolaite components in the Na-free experiments agree well with the trends observed in natural clinopyroxenes that contain significant jadeite components. This indicates that first order CMAS relations in clinopyroxene are not strongly affected by Na. Additional experiments are needed to clarify in detail the influence of Na on the incorporation of Ca-tschermak and Ca-eskolaite components in clinopyroxene.

Garnet and orthopyroxene

Garnet displays a systematic increase in grossular content with increasing pressure at a fixed temperature (Fig. 7a). At a given pressure, the grossular content increases with increasing temperature. No significant excess of Si per formula unit has been found in garnets indicating that there is no evidence for majorite component in the investigated P–T range.

Orthopyroxene displays a systematic increase of Ca and Al content with increasing temperature (Fig. 7b). As the orthopyroxene field is very small it is not possible to decipher a clear pressure effect. Orthopyroxene is so far not known to be a typical high-pressure phase in crustal rocks. However, orthopyroxene coexisting with kyanite

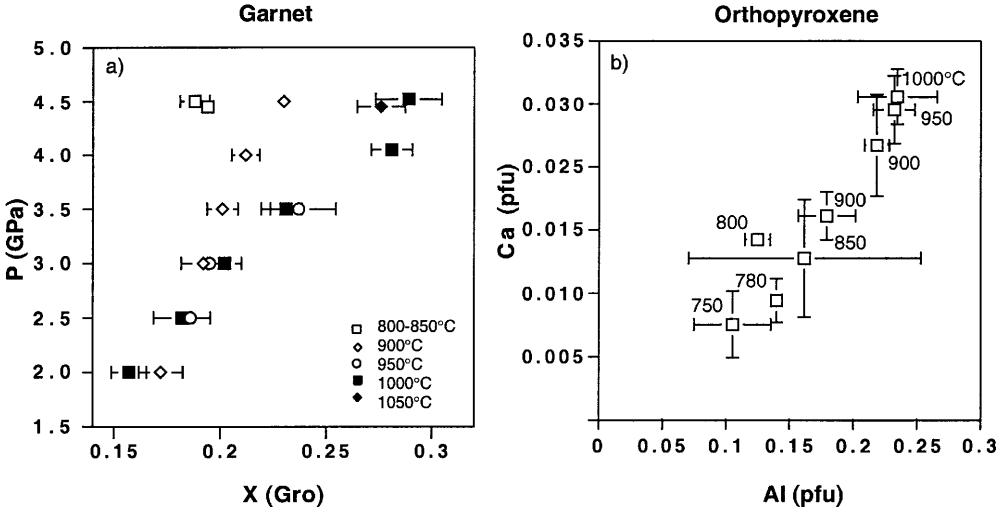

Fig. 7a. The grossular content of garnet [X (Gro) = Ca/(Mg + Ca)] increases with increasing pressure. **b** Both Al and Ca increase with increasing temperature in orthopyroxene

has been described to form in cracks in pyrope megablasts in white schist of the Dora Maira Massif (Simon and Chopin 2001), which formed well within the coesite stability field (Schertl et al. 1991). The natural orthopyroxene in equilibrium with kyanite contains typically about 3 wt% Al_2O_3, which is in the range of the experimentally grown orthopyroxenes between 750 °C (~2.6%) and 800 °C (~3.2%). These temperatures compare very well with temperatures during initial decompression of the Dora Maira Massif (Schertl et al. 1991) and suggest orthopyroxene and kyanite can be an ultrahigh-pressure assemblage in very Mg-rich rock types.

Theoretical phase relations

Theoretical phase relations based on chemography (Fig. 1) and Schreinemaker's rule can be compared with the experimental results (Fig. 2). The combination of the two methods permits the construction of a petrogenetic grid in the investigated P–T space. Eleven solid phases + a liquid phase were found in the six-component (KCMASH) system. Such a system produces 495 possible invariant points, among which most are irrelevant for the actual grid. The system can be drastically simplified by subdivision into smaller systems and by projection from phases that are in excess. All experiments are saturated in kyanite, liquid and coesite/quartz and, therefore, it is possible to project from these phases. The resulting system contains three components (KCM), eight phases and produces 56 possible invariant points. The phase relations can be further simplified by regarding the subsystem between 3.5 and 4.5 GPa and 700–900 °C. The phases coesite, kyanite, phengite, clinopyroxene and liquid occur over this P–T region whereas biotite, orthopyroxene, talc and garnet have restricted stability fields. By projecting additionally from phengite and clinopyroxene the multisystem simplifies to one component (Mg) and four phases, and the resulting grid with four invariant points is easy to construct (Fig. 8a). A more complicated subsystem exists between 2.0 and 3.5 GPa and 700–800 °C. In this subsystem it is possible to project only from the phases kyanite, quartz/coesite and liquid. Additional phases are talc, biotite, phengite, amphibole, zoisite and clinopyroxene, and this subsystem can be described by six phases and three components. The geometrical analyses of such systems has been provided by Day (1972). The chemography and the phase composition given in Fig. 1b, represent the geometry of chemography T49 of Day (1972), which can be translated to a grid with four stable and two metastable invariant points as shown in Fig. 8b. In the chosen bulk composition, 11 out of the 14 possible univariant reaction should appear in the petrogenetic grid. The subsystem involving the melting reactions of biotite and

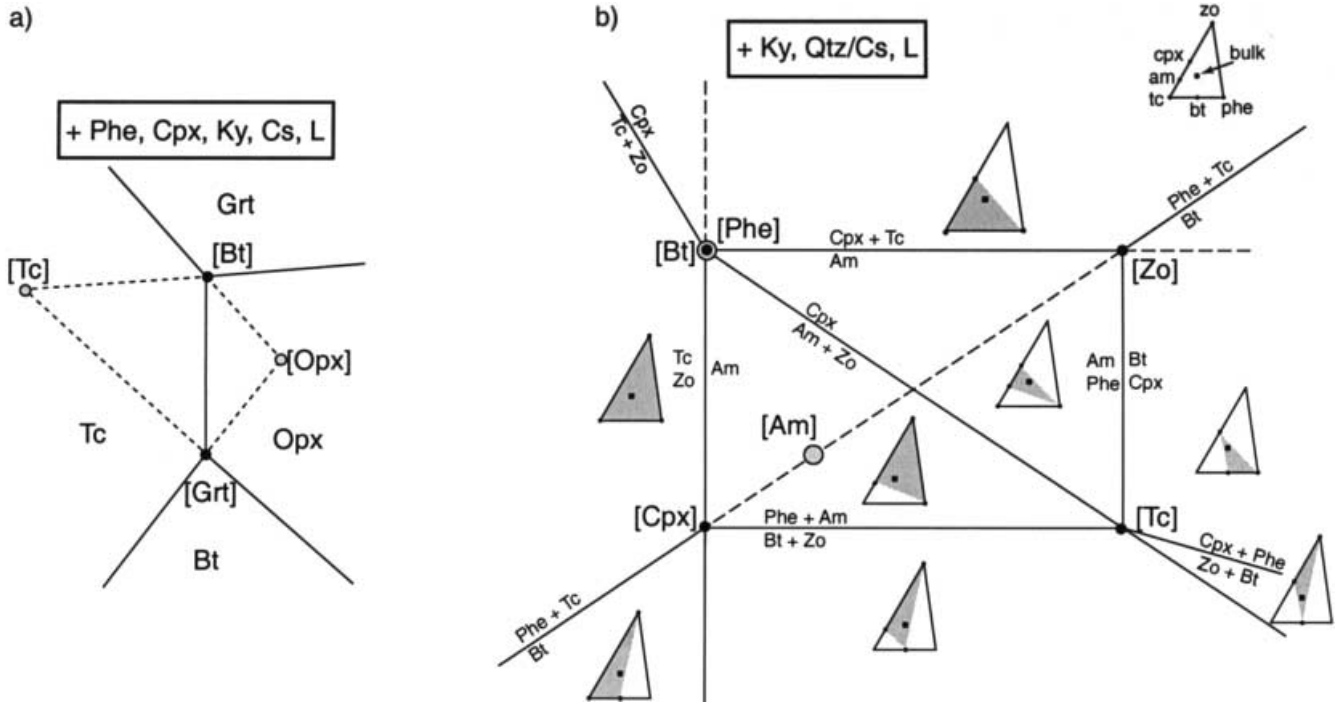

Fig. 8a,b. Geometrical analysis of phase relations in subsystems. **a** Multisystem showing the possible relations of the Mg phases after projection from phengite, clinopyroxene, kyanite, coesite and liquid. Stable (*solid*) and metastable (*dashed*) univariant lines are shown and absent phases at an invariant point are labeled with *squared brackets*. **b** Multisystem with three components and six phases after projection from kyanite, quartz/coesite and liquid. Stable invariant points (*black dots*) and metastable invariant points (*grey dots*) are labeled with the absent phase. *Black solid lines* refer to stable univariant lines that lead to a change in paragenesis whereas *dashed lines* are stable univariant lines that do not occur in the chosen bulk composition. The stable paragenesis for each field is indicated

phengite has been described in detail by Hermann and Green (2001) and is not reproduced here. In the next step, the subsystems must be oriented in P–T space, linked together and fitted to the experimental data. It was actually possible to construct a fully consistent grid that satisfies the experimental results as well as theoretical constraints (Fig. 9). Experiments that are situated in a divariant field contain five solid phases plus liquid as predicted by the phase rule for a six-component system with no degeneration. Six solid phases were observed in experiments close to univariant lines and two experiments close to invariant points contained seven solid phases. In the region above the phengite and biotite stability fields, degeneration leads to paragenesis with one phase less than in the rest of the grid (Hermann and Green 2001).

Discussion

Comparison of the KCMASH petrogenetic grid with other studies

Hoschek (1990) reported experiments up to 2.0 GPa in the KCMASH system, which can be linked to this study.

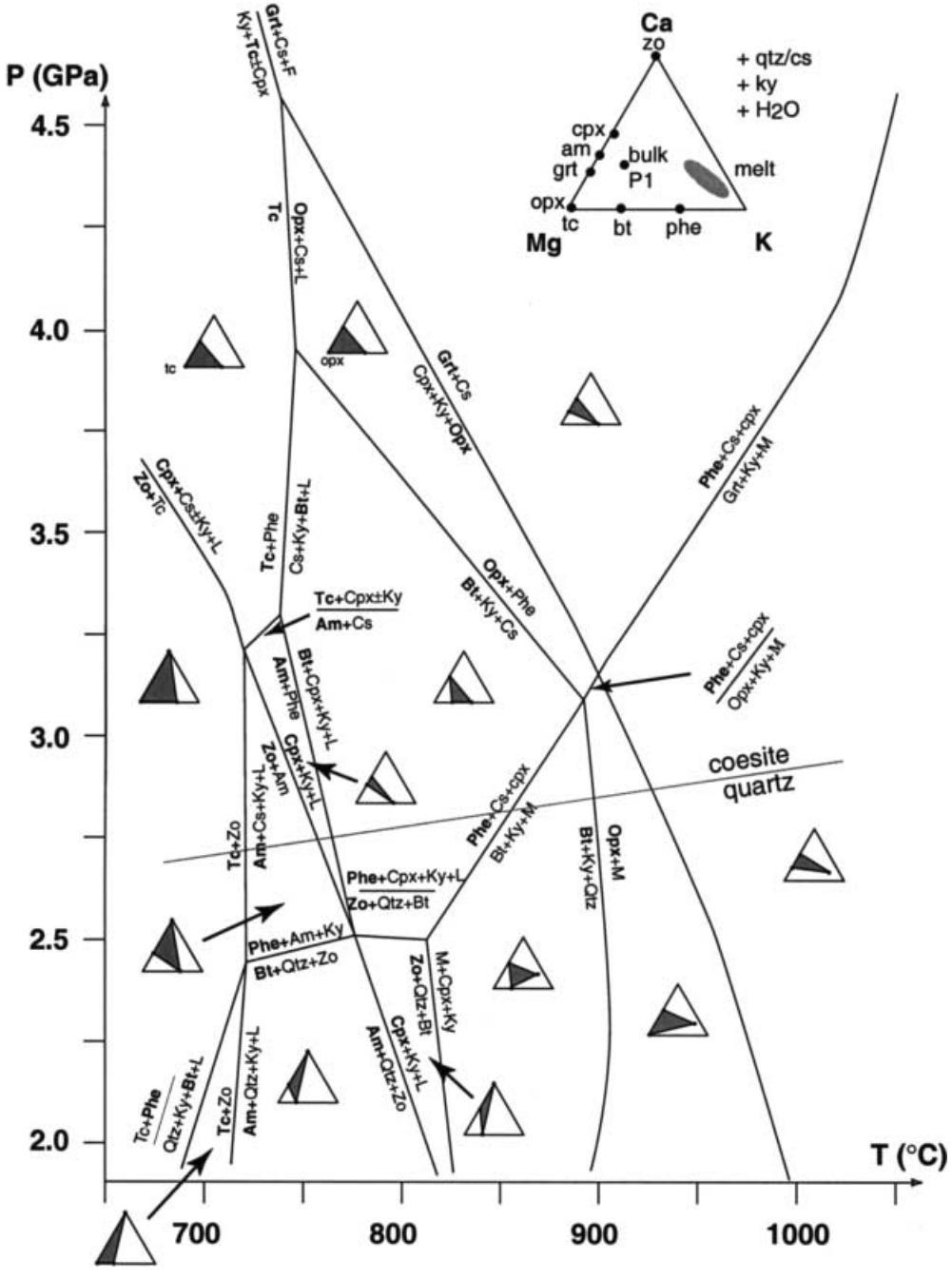

Fig. 9. Petrogenetic grid for subducted continental crust in the model system KCMASH based on the experimental results (Fig. 2), and the geometrical analyses of phase relations (Figs. 1 and 8). The phases in *bold* are exhausted along the univariant reactions as a result of the chosen bulk composition (Fig. 1). The paragenesis of each field is indicated by the chemography. The coesite–quartz transition is taken from Bohlen and Boetcher (1982). Probable changes of slopes of reactions caused by the coesite–quartz transition are beyond resolution of the data and are not shown in the diagram

He estimated the position of the invariant point involving the phases talc, biotite, phengite, zoisite, amphibole, kyanite, quartz and liquid at about 720 °C, 2.0 GPa. The temperature is identical, whereas this study suggests a slightly higher pressure of 2.4 GPa for this invariant point. At 2.0 GPa, Hoschek (1990) did not find clinopyroxene up to the highest experimental temperature of 760 °C, which is in agreement with the results presented here constraining the first appearance of clinopyroxene at ~800 °C at 2.0 GPa.

Data on the subsystems MASH, CMASH and KMASH can also be compared with the obtained experimental data. In the MSH system, the reaction

$$\mathrm{Tc} \leftrightarrow \mathrm{Opx} + \mathrm{Cs} + \mathrm{L}$$

has been reported in several studies and can be compared with the present study. This reaction has been located in the MSH system between 800 and 850 °C at 2.0–3.0 GPa (Kitahara et al. 1966; Thompson and Ellis 1994) and at 770 °C at 4.0 GPa (Pawley and Wood 1995). This is about 40–60 °C higher than the disappearance of talc in this study, which is proposed to be between 710 and 730 °C at 4 GPa (Fig. 9). A possible explanation is the difference of the bulk system used. Because Al is incorporated less in the reactant talc (0.5 wt% at 700 °C, 4.45 GPa) than in the product orthopyroxene (2.6 wt% at 750 °C, 4.0 GPa), the talc break-down reaction is probably shifted to slightly lower temperatures. Additional components, especially K and Al, will influence the liquid composition. In the KCMASH, there are much more solutes in the liquid than in the MSH system and, consequently, the H_2O activity in the liquid is expected to be lower in the KCMASH system resulting in break down of talc at a lower temperature.

The KMASH univariant reaction

$$\mathrm{Tc} + \mathrm{Phe} \leftrightarrow \mathrm{Bt} + \mathrm{Ky} + \mathrm{Qtz} + \mathrm{L}$$

has been experimentally investigated by Massone and Schreyer (1989) to be at 610 °C, 1.0 GPa to 770 °C, 2.5 GPa. Based on the set of experiments presented here, the transition is suggested to be 50 °C lower at 2.5 GPa. Because there are no compositional data available from the study of Massone and Schreyer (1989), it is difficult to compare the results directly. For example, at slightly higher temperatures (840°, 2.5 GPa) a hydrous melt in the KCMASH system contains 4.2 wt% of CaO (Hermann and Green 2001). This could lead to lower H_2O activity in the studied KCMASH compared with the KMASH system, resulting in a shift of the talc + phengite stability to lower temperatures.

Phengite and biotite are absent at one invariant point of the KCMASH subsystem (Fig. 8b) permitting a comparison with results in the CMASH system (Thompson and Ellis 1994). The topology of the univariant reactions around the invariant point proposed here is identical to the one given by Thompson and Ellis (1994). Interestingly, although the slopes of the reactions are only constrained by the phase relations and experiments (Fig. 9), they compare very well with the slopes calculated by Thompson and Ellis (1994), suggesting that the presented phase relations are in line with other studies. According to the presented data this invariant point is at ~720 °C, 3–3.2 GPa, whereas Thompson and Ellis proposed it at lower pressures of ~2.5 GPa. Amphibole is the only phase in this subsystem that can incorporate K. Therefore, it is expected that the assemblage Am + Cs has a stability at higher pressures in the KCMASH system than in the CMASH system, which is in agreement with the experimental results. Experiments by Hoschek (1995) in the CMASH system constrained the reaction

$$\mathrm{Zo} + \mathrm{Tc} \leftrightarrow \mathrm{Tr} + \mathrm{Ky} + \mathrm{Qtz} + \mathrm{L}$$

between 700 and 750 °C at 2.0 GPa, which is in perfect agreement with the results shown in Fig. 9.

The high-pressure stability field of orthopyroxene found in this study cannot be explained by the problem of garnet nucleation, as demonstrated by experiments seeded with garnet. The transition of orthopyroxene to garnet was found to be sluggish and occurred over a temperature range of about 50 °C. This is in agreement with KMASH synthesis experiments of Massone and Szpurzka (1997), where orthopyroxene occurs as a minor phase together with garnet at similar P–T conditions. On the basis of experiments in the MAS system, Hensen and Essene (1970) suggested that the reaction of kyanite + orthopyroxene to pyrope + quartz occurs at 1.8 GPa, 1,000 °C, which is very close to the proposed lower pressure end of the garnet + quartz stability in the investigated system (Fig. 9).

Thompson and Ellis (1994) report garnet at much lower P–T conditions than the present study. This is most likely a function of the chosen bulk composition. Although their bulk is originally quartz saturated, the addition of 15–25% of H_2O led to high amounts of dissolved Si and complete dissolution of quartz. The stable paragenesis of garnet + coesite in similar bulk rock compositions is present at similar conditions in the P–T space. Additionally, garnet and clinopyroxene in experiments buffered by kyanite and garnet display very similar phase compositions to the ones reported here.

In summary: the reported KCMASH petrogenetic grid (Fig. 9) is generally in agreement with reactions and parageneses reported in studies of related subsystems. It has to be tested to what extent discrepancies of about 50 °C in the position of dehydration reactions are related to different activities in H_2O caused by different amounts of solutes in the fluid. Although the petrogenetic grid was constructed for rocks containing kyanite and quartz/coesite, it bears important information for other bulk rock systems. At every invariant point shown in Fig. 9 there are also reactions relevant for kyanite- and quartz–coesite-free rocks. The slopes of these reactions are constrained by the position of the experimentally determined reactions and Schreinemaker's rule.

High-pressure parageneses in subducted crust

The investigated system permits establishment of systematic phase relations in a model crustal composition. However, natural rocks contain significant amounts of Na and Fe, which complicate the phase relations. In this section, the experimental results are first applied to special rocks with very close chemical composition to the investigated system. Then, the effect of Na and Fe on the phase relations are discussed on the basis of existing experiments in natural systems and eclogite facies metapelites and metagranitoids.

Whiteschists from the Dora Maira Massif have a bulk rock composition that is very close to the KMASH system and permits a direct comparison with those experiments. The whiteschists contain coesite and document the reaction Ky + Tc -> Grt + Cs + F (Schertl et al. 1991). According to the experiments, this reaction occurs at ~750 °C and well within the coesite stability field (Fig. 9). The temperature estimate is in very good agreement with garnet–clinopyroxene thermometry from eclogites of the same unit (Kienast et al. 1991). Most of natural white-schists display different amounts of Fe and contain divariant paragenesis garnet, kyanite, phengite, talc and coesite as, for example, in the Kokchetav Massif in Kazakhstan (Zhang et al. 1997; Parkinson 2000). Because garnet preferentially incorporates Fe compared with talc (Zhang et al. 1997), talc disappears at lower temperatures than 750 °C, dependent on the Fe/Mg ratio of the bulk rock. The presence of talc in the Kokchetav whiteschists provides evidence that peak metamorphic temperatures were below 750 °C. Hence, these rocks experienced much lower temperatures than neighbouring diamondiferous rocks, which were metamorphosed at about 950 °C (Shatsky et al. 1995; Zhang et al. 1997; Hermann and Green 2001).

The introduction of Na and Fe does not produce additional UHP phases. Univariant reactions in the KCMASH system will diverge in trivariant fields and, hence, the appearance and disappearance of phases is not only caused by discontinuous reactions, but is also bulk rock dependent. Na substitutes mainly for Ca and, therefore, this influences the stability fields of the Ca phases found in the petrogenetic grid. Experiments in granitic (Green and Lambert 1965) and pelitic (Patiño Douce and McCarthy 1998) compositions demonstrate that plagioclase could be stable at the high temperature/low pressure end of the investigated grid. However, at temperatures below 1,000 °C, plagioclase was not found to be stable above 2.3 GPa. Na probably decreases the stability field of talc + zoisite with respect to omphacite + coesite + kyanite because zoisite is Na-free. It is more difficult to establish the effect of Na and Fe on the transition from amphibole to omphacite. Experiments in basaltic to andesitic compositions indicate that amphibole is not stable above ~2.5 GPa (Poli and Schmidt 1995) and, hence, the introduction of Fe and Na stabilizes the higher pressure assemblage omphacite + garnet rather than amphibole. Consequently, it is expected that clinopyroxene is the main Na phase in UHP conditions. The introduction of Fe affects all Mg-bearing phases and increases the stability field of garnet, which preferentially incorporates Fe. The small orthopyroxene field, present in the pure Mg system (Fig. 9), will disappear and biotite is consumed along the continuous reaction bt + ky + cs ↔ grt + phe. The position of complete biotite consumption in the presence of kyanite and coesite/quartz is thus a function of bulk rock composition, especially of the Mg# (Mg/Mg + Fe). Based on experiments in a natural Ca-poor system, Vielzeuf and Holloway (1988) suggested that this reaction occurs at ~1.8 GPa for a bulk Mg# of 0.5 (see Fig. 10). Green and Hellman (1982) found the paragenesis grt + phe + ky ± qtz/cs from 2.0–3.5 GPa in hydrous experiments of phengite (Mg# = 0.67) + quartz. Therefore, the para-

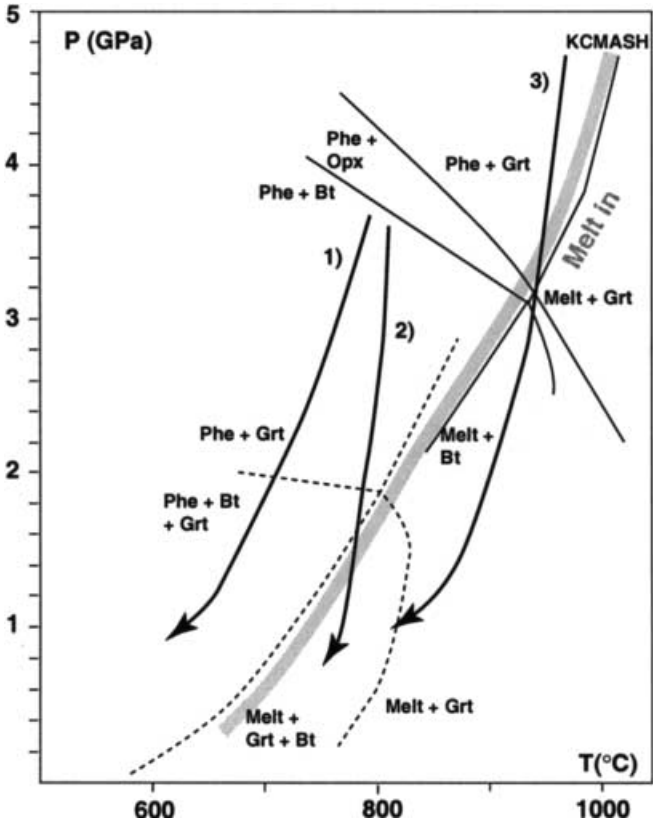

Fig. 10. Phase relations in the KCMASH system (*solid lines*; this study) and in a natural system with Mg# = 0.5 (*dashed lines*; Vielzeuf and Holloway 1988). Note the enlargement of the stability field garnet + phengite to lower pressures by the introduction of Fe. The position of fluid-absent melting of mica-bearing rocks is fundamental for the retrograde overprint of subducted continental crust. *1* Cooling during exhumation is documented in the Dora Maira Massif (Schertl et al. 1991) and occurs most probably in thin sheets of UHP rocks (< 1 km thickness). *2* Thicker sheets of UHP rocks are probably not able to lose the internal heat during fast exhumation and follow an near isothermal decompression curve as the Sulu UHP rocks (Nakamura and Hirajima 2000). *3* Most of the exhumation path of the diamondiferous rocks from the Kokchetav Massif is situated within the partial melting field. Therefore, only refractory phases such as garnet, kyanite and zircon may survive retrogression due to partial melting (Hermann et al. 2001)

genesis grt + phe + qtz/coe + ky ± cpx can be stable from the amphibolite–eclogite facies transition up to very high conditions of at least 4.5 GPa and 1,000 °C in pelitic compositions. In fact, Ono (1998) found this assemblage (without kyanite) up to conditions of 1,200 °C and 6.0 GPa. The influence of Na and Fe on the phengite-melting reaction is discussed by Hermann and Green (2001).

A grt + phe + qtz/coe + ky ± cpx paragenesis for pelitic rocks has been reported from several localities in the Alps, where interlayered mafic rocks are proof of eclogite facies conditions: Dora Maira Massif (3.5 GPa, 750 °C; Chopin 1984; Compagnoni et al. 1995), Adula nappe (2.0–2.5 GPa, 650 °C; Meyre et al. 1999), Cima Lunga unit (2.5–3.0 GPa, 800 °C; Heinrich 1986). The presence of this same paragenesis over a wide range of metamorphic conditions is in agreement with the experimental results. Recently, Carswell et al. (2000) proposed that the gneisses and schists of the Dabie–Shan in China experienced UHP metamorphism, together with intercalated mafic and ultramafic rocks. From textural evidence they conclude that the eclogite facies paragenesis consists of garnet, phengite, quartz (no coesite found yet) and minor kyanite. They suggest that allanite was stable at peak metamorphic conditions and was later rimed by clinozoisite. According to the presented experimental data, this feature would be consistent with an UHP origin of the schists beyond the stability of zoisite (Fig. 9). In the experiments, traces of allanite have been found well above the stability of zoisite (Table 2, Fig. 3b) because the added trace elements La and Ce stabilize allanite.

The experiments of this study were conducted in H_2O-saturated conditions, which is a prerequisite to attain equilibrium at the low experimental temperatures (e.g. Poli and Schmidt 1995). In H_2O-saturated conditions, phengite, and to a lesser extent biotite, are the stable K-phases (Fig. 9). This is in agreement with H_2O-saturated experiments in K-MORB composition where phengite is the stable K phase up to ~9 GPa, 1,000 °C (Schmidt 1996). Experiments in a natural muscovite schist in slightly H_2O-undersaturated conditions (Patiño Douce and McCarthy 1998) produced K-feldspar that coexists with phengite at UHP conditions. Austrheim (1998) compiled data from several eclogite facies terrains in which metastable anhydrous low pressure assemblages occur. These assemblages are explained by a lack of fluid at high-pressure conditions. It is suggested that equilibrium parageneses in natural eclogite facies rocks are generally restricted to zones formed under H_2O-saturated conditions and hence H_2O-saturated experiments are suitable to constrain UHP metamorphism of subducted crust.

In summary, the experiments demonstrate that rocks such as phengite talc schists, phengite garnet schists and, to a lesser extent biotite phengite schists, are stable in pelitic to granitic compositions at UHP conditions. Such parageneses do not significantly differ from the ones formed in amphibolite facies conditions. Thus, it is much more difficult to recognize eclogite facies felsic rocks than mafic rocks where eclogite facies conditions are documented by the characteristic paragenesis of omphacite and garnet. One common feature for mafic and felsic rocks is the absence of feldspars in H_2O-saturated systems. Although K-feldspar occurs in H_2O-undersaturated conditions, plagioclase is never stable in UHP conditions

Hydration and dehydration of subducted crust

The experiments revealed that for a wide range of pressures at temperatures below 800 °C, there are two or more coexisting hydrous phases. The experiments further indicate that the capacity of quartz + kyanite-bearing rocks to store H_2O is strongly dependant on Mg# and K content. In Mg-rich rocks this capacity is constrained by the stability of talc. K-rich rocks are most suitable to transport H_2O at great depth because of the stability of phengite, whereas Ca-rich hydrous minerals such as zoisite and amphibole break down to clinopyroxene at much lower pressure (Fig. 9). Rocks with MORB composition contain less than 0.5 wt% H_2O at $T > 650$ °C and $P > 3.0$ GPa (Schmidt and Poli 1998). At the same conditions, metapelites are likely to contain 1–2 wt% of H_2O, depending on the amount of talc and mica with respect to anhydrous phases. At temperatures below 600–650 °C, ultramafic rocks are the most important H_2O carrier (Ulmer and Trommsdorff 1995). However, beyond the serpentine and chlorite stability fields, i.e. at conditions $T > 800$ °C and $P > 3.0$ GPa, ultramafic rocks are dry (Schmidt and Poli 1998) and H_2O is only stored in crustal rock compositions. As Schmidt and Poli (1998) pointed out, the amount of H_2O in subducted sediments is not significant because of the low volume percentage of sediments in the down-going slab. However, in zones of continental subduction. such as the Dora Maira Massif or the Kokchetav Massif, significant amounts of H_2O can be carried to mantle depth by crustal rocks.

There is a fundamental difference between the behaviour of subducted oceanic and continental crust in terms of dehydration during subduction. Basalts are likely to be hydrated during hydrothermal alteration at the ocean floor and the covering oceanic sediments contain water-saturated assemblages, which then progressively lose H_2O during burial (Schmidt and Poli 1998). Apart from completely hydrated sediments, the continental crust also consists of granite and basement rocks, which often contain less H_2O at the beginning of subduction than during peak metamorphic conditions. The main reason for this behaviour is the K-phase in crustal rocks. K-feldspar is absent in subducted oceanic crust, but is a common mineral in continental crust and occurs in granites, greywackes and amphibolite facies gneisses. At high pressure, phengite is the stable K phase in the presence of a fluid and, consequently, the above mentioned rocks hydrate rather than dehydrate at

eclogite facies conditions. Often the amount of H_2O available is not enough to completely hydrate granitic bodies at depth and, therefore, K-feldspar can be part of eclogite facies continental crust in H_2O-undersaturated conditions. K-feldspar in UHP rocks has been described from a coronitic granitic body in the Dora Maira Massif, which is replaced by phengite in the more hydrated parts (Biino and Compagnoni 1992). The possibility of hydration at UHP conditions is important for the correct interpretation of fluid inclusions of subducted crustal materials. Although dehydration reactions should produce low saline fluids/melts (but with significant amounts of dissolved K, Al and Si), fluids trapped from hydration reactions can be highly saline because the hydrous phases preferentially incorporate OH with respect to Cl (Volfinger et al. 1985). Consequently, the continuous reaction of a H_2O-rich fluid with K-feldspar to produce phengite will lead to a passive enrichment of Cl and a highly saline brine at a final stage of hydration.

Preservation of UHP metamorphism in the subducted crust

Figure 10 summarizes the region where micas are stable from this study in the synthetic KCMASH system and in a natural system for pelites with Mg# of 0.5, by Vielzeuf and Holloway (1988). The fluid-absent melting of phengite displays a positive slope and is fundamental for the question of whether or not UHP parageneses in crustal rocks survive during exhumation. UHP rocks from the Dora Maira Massif reached peak temperatures of 750 °C at 3.5–4.0 GPa and were cooled during exhumation to 600 °C at 1.0 GPa (Schertl et al. 1991). Therefore, the whole retrograde P–T path was situated well within the stability fields of micas, and UHP parageneses are still preserved in low strain regions. In contrast, UHP rocks from the Sulu region in China display a granulite facies overprint indicating near isothermal decompression at ~800 °C (Nakamura and Hirajima 2000). Such isothermal decompression should produce partial melting during phengite break down and, consequently, leads to a complete recrystallization of the felsic rocks. Even higher temperatures are documented in the Kokchetav Massif with 950 °C, $P > 4.3$ GPa and slight cooling during decompression to 800 °C and 1.0 GPa (Zhang et al. 1997; Hermann et al. 2001). Most of the decompression path is situated within the partial melting field and relics of UHP minerals are mainly found as inclusions within zircon (Katayama et al. 2000b; Hermann et al. 2001) or garnet (Shatsky et al. 1995). Hence, the two parameters, which are of first-order importance for the preservation of UHP parageneses in subducted crust, are low peak temperature and cooling during exhumation. Mafic rocks, which are often intercalated with pelites and orthogneisses in crustal rocks, display a different behaviour during exhumation. Their peak mineralogy is stable as long as there is no fluid available during decompression. On the basis of field relations in the central Alps, Heinrich (1982) proposed that the different behaviour of felsic and mafic rocks during exhumation could explain why eclogite facies mafic lenses are embedded in upper amphibolite facies felsic gneisses. The experimental work presented here supports this hypothesis.

Density and the exhumation of subducted continental crust

The experiments revealed that the most important rock types of subducted continental crust consist of garnet ($\rho = 4.0$ g/cm^3), kyanite ($\rho = 3.59$ g/cm^3), phengite ($\rho = 2.81$ g/cm^3), coesite ($\rho = 2.92$ g/cm^3), clinopyroxene ($\rho = 3.31$ g/cm^3) and, at low temperature, talc ($\rho = 2.78$ g/cm^3). For an average granitic composition there is 25% phengite, 25% clinopyroxene, 50% of coesite and traces of garnet and kyanite resulting in a density of about 3.0 g/cm^3 at room conditions. An average pelite composition results in 30% phengite, 10% jadeite, 20% garnet, 5% kyanite and 35% coesite with a density of about 3.3 g/cm^3. Therefore, it is likely that the average density of the subducted continental crust is around 3.15 g/cm^3, which is significantly lower than average density of the mantle rocks at the same depth. Subducted continental crust, thus, is buoyant at mantle depths and might lead to termination of subduction (Cloos 1993) and might provide a driving force for exhumation of UHP rocks (Platt 1993; Ernst 1999). Buoyancy could be one of the major reasons for fast exhumation of UHP continental crust, which can act at a speed of several centimetres per year (Rubatto and Hermann 2001).

Metamorphic, orogenic garnet peridotites and UHP eclogites are always associated with gneisses that are generally of continental origin (Coleman and Wang 1995). It suggests that buoyant subducted continental crust could be an important carrier for garnet peridotites and eclogites, which have a density higher than mantle rocks.

Conclusions

There are probably two main reasons for the scarcity of reported UHP occurrences in continental crust. (1) Synthesis experiments demonstrated that paragenesis phengite, coesite, kyanite, clinopyroxene, garnet is stable at UHP conditions. Apart from omphacite (and coesite, which transforms to quartz), all the other minerals are also stable at amphibolite facies conditions making the recognition of UHP rocks difficult. (2) In order to preserve the UHP paragenesis, rocks must stay within the white mica stability during exhumation. Near isothermal decompression at 700–800 °C leads to phengite melting and consequently to a complete recrystallization of the rocks. This problem is probably related to the size of the

exhumed body of continental crust. Small bodies (less than 1 km thickness) are able to cool during fast exhumation on top of the slab, hence preserving the UHP mineralogy, while large bodies follow an adiabatic path with only little cooling. The phase relations and the compositional trends of fully buffered minerals reported in this study contribute to the recognition of UHP metamorphism in continental crust and provide constraints on prograde and retrograde evolutions documented in zoned minerals.

Subducted continental crust is buoyant to a much greater depth than subducted oceanic crust with respect to mantle rocks. Thus, UHP continental crust is likely to get exhumed once it is detached from the slab and this permits insight into processes that occur at a critical depth for subduction zone magmatism, i.e. at depths of 100–150 km. Continental crust is able to retain a greater amount of H_2O at UHP conditions above 800 °C than oceanic crust or mantle rocks.

Acknowledgements I would like to thank W.O. Hibberson and D. Scott for technical assistance in the high-pressure laboratory and the crew from the Electron Microscope Unit (ANU) for help with the SEM. Comments from M.W. Schmidt, D.J. Ellis, D.H. Green, S. Harley and D. Rubatto, and constructive reviews of S. Poli and A. Patiño Douce helped to improve the manuscript. I thank J. Hoefs for his editorial handling. This work was financially supported by the Schweizerischer Nationalfonds ('Nachwuchsstipendium') and the Australian Research Council.

References

Austrheim H (1998) Influence of fluid and deformation on metamorphism of the deep crust and consequences for the geodynamics of subduction zones. In: Hacker BR, Liou JG (eds) When continents collide: geodynamics and geochemistry of ultrahigh-pressure rocks. Kluwer, Dordrecht, pp 297–323

Biino G, Compagnoni R (1992) Very high-pressure metamorphism of the Brossasco coronite metagranite, southern Dora Maira Massif, Western Alps. Schweiz Mineral Petrogr Mitt 72:347–363

Bohlen SR, Boetcher AL (1982) The quartz–coesite transformation: a precise determination and the effects of other components. J Geophys Res 87:7073–7078

Carswell DA, Dawson JB, Gibb FGF (1981) Equilibration condition of upper mantle eclogites: implications for kyanite bearing and diamondiferous varieties. Mineral Mag 44:79–89

Carswell DA, O'Brien PJ, Wilson RN, Zhai M (1997) Thermobarometry of phengite-bearing eclogites in the Dabie Mountains of central China. J Metamorph Geol 15:239–252

Carswell DA, Wilson RN, Zhai M (2000) Metamorphic evolution, mineral chemistry and thermobarometry of schists and orthogneisses hosting ultra-high pressure eclogites in the Dabieshan of central China. Lithos 52:121–155

Chopin C (1984) Coesite and pure pyrope in high grade blueschists of the western Alps: a first record and some consequences. Contrib Mineral Petrol 86:107–118

Cloos M (1993) Lithospheric buoyancy and collisional orogens: Subduction of oceanic plateaus, continental margins, island arcs, spreading ridges, and seamounts. Geol Soc Am Bull 105:715–737

Coleman RG, Wang X (1995) Overview of the geology and tectonics of UHPM. In: Coleman RG, Wang X (eds) Ultrahigh-pressure metamorphism. Cambridge University Press, Cambridge, pp 1–32

Compagnoni R, Hirajima T, Chopin C (1995) Ultra-high-pressure metamorphic rocks in the Western Alps. In: Coleman RG, Wang X (eds) Ultrahigh pressure metamorphism. Cambridge University Press, Cambridge, pp 206–243

Day HW (1972) Geometrical analysis of phase equilibria in ternary systems of six phases. Am J Sci 272:711–734

Domanik KJ, Holloway JR (1996) The stability of phengitic muscovite and associated phases from 5.5 to 11 GPa: implications for deeply subducted sediments. Geochim Cosmochim Acta 60:4133–4150

Domanik KJ, Holloway JR (2000) Experimental synthesis and phase relations of phengitic muscovite from 6.5 to 11 GPa in a calcareous metapelite from the Dabie Mountains, China. Lithos 52:51–77

Ernst WG (1999) Metamorphism, partial preservation, and exhumation of ultrahigh-pressure belts. Island Arc 8:125–153

Eskola P (1920) The mineral facies of rocks. Norsk Geol Tidsskr 6:143–194

Green DH, Lambert IB (1965) Experimental crystallization of anhydrous granite at high pressures and temperatures. J Geophys Res 70:5259–5268

Green DH, Ringwood AE (1967) An experimental investigation of the gabbro to eclogite transformation and its petrological applications. Geochim Cosmochim Acta 31:767–833

Green TH, Hellman PL (1982) Fe–Mg partitioning between coexisting garnet and phengite at high pressure, and comments on a garnet–phengite geothermometer. Lithos 15:253–266

Harley SL, Carswell DA (1995) Ultradeep crustal metamorphism: a prospective view. J Geophys Res 100:8367–8380

Heinrich CA (1982) Kyanite–eclogite to amphibolite facies evolution of hydrous mafic and pelitic rocks, Adula nappe, Central Alps. Contrib Mineral Petrol 81:30–38

Heinrich CA (1986) Eclogite facies regional metamorphism of hydrous mafic rocks in the Central alpine Adula nappe. J Petrol 27:123–154

Hensen BJ, Essene EJ (1970) Stability of pyrope–quartz in the system $MgO–Al_2O_3–SiO_2$. Contrib Mineral Petrol 30:72–83

Hermann J, Green DH 45 (2001) Experimental constraints on high pressure melting in subducted crust. Earth Planet Sci Lett 188:149–168

Hermann J, Rubatto D, Korsakov A, Shatsky VS (2001) Multiple zircon growth during fast exhumation of diamondiferous, deeply subducted continental crust (Kokchetav Massif, Kazakhstan). Contrib Mineral Petrol 141:66–82

Hoschek G (1990) Melting and subsolidus reactions in the system $K_2O–CaO–MgO–Al_2O_3–SiO_2–H_2O$: experiments and petrologic application. Contrib Mineral Petrol 105:353–362

Hoschek G (1995) Stability relations and Al content of tremolite and talc in CMASH assemblages with kyanite + zoisite + quartz + H_2O. Eur J Mineral 7:353–362

Huang WL, Wyllie PJ (1973) Melting relations of muscovite–granite to 35 kbar as a model for fusion of metamorphosed subducted oceanic sediments. Contrib Mineral Petrol 42:1–14

Katayama I, Parkinson CD, Okamoto K, Nakajima Y, Maruyama S (2000a) Supersilic clinopyroxene and silica exsolution in UHPM eclogite and pelitic gneiss from the Kokchetav Massif, Kazakhstan. Am Mineral 85:1368–1374

Katayama I, Zayachkovsky AA, Maruyama S (2000b) Prograde pressure–temperature records from inclusions in zircons from the ultrahigh-pressure–high pressure rocks of the Kokchetav Massif, northern Kazakhstan. Island Arc 9:417–427

Kienast JR, Lombardo B, Biino G, Pinardon JL (1991) Petrology of very high-pressure eclogitic rocks from the Brossasco–Isasca Complex, Dora Maira Massif, Italian Western Alps. J Metamorph Geol 9:19–34

Kitahara S, Takenouchi S, Kennedy GC (1966) Phase relation in the system $MgO–SiO_2–H_2O$ at high temperatures and pressures. Am J Sci 264:223–233

Konzett J, Ulmer P (1999) The stability of hydrous potassic phases in ilherzolitic mantle – an experimental study to 9.5 GPa in simplified and natural bulk compositions. J Petrol 40: 629–652

Massone HJ, Schreyer W (1987) Phengite geobarometry based on the limiting assemblage with K-feldspar, phlogopite and quartz. Contrib Mineral Petrol 96:212–224

Massone HJ, Schreyer W (1989) Stability field of the high-pressure assemblage talc + phengite and two new phengite barometers. Eur J Mineral 1:391–410

Massone HJ, Szpurzka Z (1997) Thermodynamic properties of white micas on the basis of high-pressure experiments in the systems K_2O–MgO–Al_2O_3–SiO_2–H_2O and K_2O–FeO–Al_2O_3–SiO_2–H_2O. Lithos 41:229–250

Meyre C, De Capitani C, Zack T, Frey M (1999) Petrology of high-pressure metapelites from the Adula Nappe (Central Alps, Switzerland). J Petrol 40:199–213

Nakamura D, Hirajima T (2000) Granulite-facies overprinting of ultrahigh-pressure metamorphic rocks northeastern Su-Lu region, eastern China. J Petrol 41:563–582

Nichols GT, Wyllie PJ, Stern CR (1994) Subduction zone melting of pelagic sediments constrained by melting experiments. Nature 371:785–788

Ono S (1998) Stability limits of hydrous minerals in sediment and mid-ocean ridge basalt compositions: implications for water transport in subduction zones. J Geophys Res 103:18253–18267

Parkinson CD (2000) Coesite inclusions and prograde compositional zonation of garnet in white schist of the HP–UHPM Kokchetav Massif Kazakhstan: a record of progressive UHP metamorphism. Lithos 52:215–233

Patiño Douce AE, McCarthy TC (1998) Melting of crustal rocks during continental collision and subduction. In: Hacker BR, Liou JG (eds) When continents collide: geodynamics and geochemistry of ultrahigh-pressure rocks. Kluwer, Dordrecht, pp 27–55

Pawley AR, Wood BJ (1995) The high-pressure stability of talc and 10-Å phase: storage sites for H_2O in subduction zones. Am Mineral 80:998–1003

Platt JP (1993) Exhumation of high pressure rocks: a review of concepts and processes. Terra Nova 5:119–133

Poli S, Schmidt MW (1995) H_2O transport and release in subduction zones: experimental constraints on basaltic and andesitic systems. J Geophys Res 100:22299–23314

Rubatto D, Hermann J (2001) Exhumation as fast as subduction? Geology 29:3–6

Sato K, Katsura T, Ito E (1997) Phase relations of natural phlogopite with and without enstatite up to 8 GPa: implication for mantle metasomatism. Earth Planet Sci Lett 146:511–526

Schertl H-P, Schreyer W, Chopin C (1991) The pyrope–coesite rocks and their country rocks at Parigi, Dora Maira Massif, Western Alps: detailed petrography, mineral chemistry and PT path. Contrib Mineral Petrol 108:1–21

Schmädicke E, Müller WF (2000) Unusual exsolution phenomena in omphacite and partial replacement of phengite by phlogopite + kyanite in an eclogite from the Erzgebirge. Contrib Mineral Petrol 139:629–642

Schmidt MW (1996) Experimental constraints on recycling of potassium from subducted oceanic crust. Science 272:1927–1930

Schmidt MW, Poli S (1998) Experimentally based water budgets for dehydrating slabs and consequences for arc magma generation. Earth Planet Sci Lett 163:361–379

Schreyer W (1988) Experimental studies on metamorphism of crustal rocks under mantle pressures. Mineral Mag 52:1–26

Schulze DJ, Valley JW, Spicuzza MJ (2000) Coesite eclogites from the Roberts Victor kimberlite, South Africa. Lithos 54:23–32

Shatsky VS, Sobolev NV, Vavilov MA (1995) Diamond-bearing metamorphic rocks of the Kokchetav Massif (northern Kazakhstan). In: Coleman RG, Wang X (eds) Ultrahigh pressure metamorphism. Cambridge University Press, Cambridge, pp 427–455

Simon G, Chopin C (2001) Enstatite–sapphirine crack-related assemblages in ultrahigh-pressure pyrope megablasts, Dora Maira Massif, western Alps. Contrib Mineral Petrol 140:422–440

Sobolev NV, Shatsky VS (1990) Diamond inclusions in garnets from metamorphic rocks: a new environment for diamond formation. Nature 343:742–746

Stern CR, Wyllie PJ (1973) Melting relations of basalt–andesite–rhyolithe–H_2O and a pelagic red clay at 30 kb. Contrib Mineral Petrol 42:313–323

Thompson AB, Ellis DJ (1994) CaO + MgO + Al_2O_3 + SiO_2 + H_2O to 35 kbar: amphibole, talc, and zoisite dehydration and melting reactions in the silica-excess part of the system and their possible significance in subduction zones, amphibolite melting, and magma fractionation. Am J Sci 294:1229–1289

Ulmer P, Trommsdorff V (1995) Serpentine stability to mantle depths and subduction-related magmatism. Science 268: 858–861

Ulmer P, Trommsdorff V (1999) Phase relations of hydrous mantle subducting to 300 km. In: Fei Y, Berthka CM, Mysen B (eds) Mantle petrology: field observations and high pressure experimentation. A tribute to Francis R. (Joe) Boyd. Geochemical Society, Special Publication, pp 259–281

Vielzeuf D, Holloway JR (1988) Experimental determination of the fluid-absent melting relations in the pelitic system. Contrib Mineral Petrol 98:257–276

Volfinger M, Robert J-L, Vielzeuf D, Neiva AMR (1985) Structural control of the chlorine content of OH-bearing silicates (micas and amphiboles). Geochim Cosmochim Acta 49:37–48

Yamamoto K, Akimoto SI (1977) The system MgO–SiO_2–H_2O at high pressures and temperatures – stability field for hydroxyl-chondrodite, hydroxyl-clinohumite and 10 Å-phase. Am J Sci 277:288–312

Zhang RY, Liou JG, Ernst WG, Coleman RG, Sobolev NV, Shatsky VS (1997) Metamorphic evolution of diamond-bearing and associated rocks from the Kokchetav Massif, Northern Kazakhstan. J Metamorph Geol 15:479–496

View publication stats